Pergamon

Int. J. Solids Structures Vol. 35, Nos. 1–2, pp. 19–31, 1998

0020–7683/98 $19.00 + .00

PII: S0020–7683(97)00058–9

DELAMINATION GROWTH DURING PRE- AND POST-BUCKLING PHASES OF DELAMINATED COMPOSITE LAMINATES

IZHAK SHEINMAN,† GEORGE A. KARDOMATEAS‡ and ASSIMINA A. PELEGRI

School of Aerospace Engineering, Georgia Institute of Technology, Atlanta, GA 30332-0150, U.S.A.

(*Received* 25 *January* 1996; *in revised form* 22 *January* 1997)

Abstract—The delamination growth during the pre- or post-buckling phases in composites with a single delamination (one-dimensional model) is investigated. For that purpose, a general nonlinear analysis, using variational principle, with a new set of relations for the decomposition of the total energy release rate, is used for an arbitrary one-dimensional composite laminate structure. A computer code is developed and used for the parametric study of delamination growth during buckling. The effects of a wide range of parameters, like imperfection, layup, location of delamination, theory type and length-to-thickness ratio, were intensively studied. It is found that a dominant parameter, in terms of the level of energy release rate, is the length-to-thickness ratio.

INTRODUCTION

Delamination onset and growth in compressively loaded composite laminated structures is one of the most severe problems concerning the confident use of laminate composites. It may significantly impair the load carrying-capacity due to local buckling (see, for example, Sheinman *et al.*, 1989) and due to crack propagation (Chai *et al.*, 1981). Local buckling itself does not imply the ultimate load, and usually, if the delamination does not grow, the laminate is capable of carrying on in the post-buckling phase under higher loading (Sheinman and Soffer, 1991). With delamination growth, the load carrying capacity is reduced further and this detracts from the high potential of composites. The complexity of the coupling of delamination growth and buckling motivates the need for more accurate modeling for predicting the behavior.

Both topic subjects of crack propagation and post-buckling behavior, have recently received tremendous attention in the literature (see for example Hutchinson and Suo (1992), Suo (1990), Sallan and Simitses (1985), and Kardomateas (1993, 1994)). Most studies were confined to homogeneous isotropic materials, some to orthotropic with a single fiber orientation, very few to anisotropic and almost none to laminate composites with an arbitrary stacking sequence. Due to the complexity of the subject, the few papers which deal with non-homogeneous laminate composites use the numerical finite element procedure (see for example O'Brien (1982), Whitcomb (1989) and Kutlu (1992)). It is apparent that the problem of non-linear behavior with delamination growth is still open for exploration.

Analysis of growth of delamination is basically governed by the Griffith criterion, which postulates that the energy release rate is the dominant parameter controlling delamination growth. A model depending on a mode-dependent fatigue delamination growth law was applied, and shown to correlate with the fatigue delamination growth data from cyclic compression tests, in Kardomateas *et al.* (1995). Recently, Sheinman and Kardomateas (1997), developed a set of relations (with no use of three-dimensional analysis), for the energy release rate and the Mode I and Mode II stress intensity factors, which can be applicable to laminates with an arbitrary stacking sequence.

† On Sabbatical leave—Technion Israel Institute of Technology.
‡ Author to whom correspondence should be addressed.

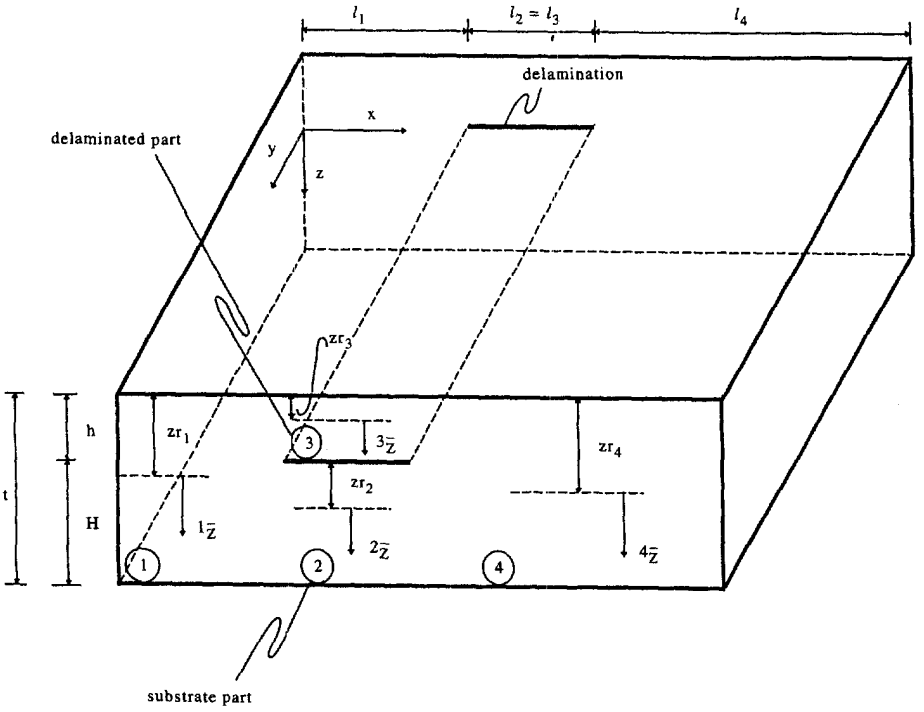

Fig. 1. Laminate with delamination through the width—geometry and sign convention.

In the present paper, these new relations of Sheinman and Kardomateas (1997), are used with a general nonlinear analysis for singly delaminated composites. An extensive parametric study of delamination growth during the pre- and post-buckling phases is conducted. For that purpose a non-linear analysis, based basically on Sheinman and Soffer (1991), is further extended for the general case of a laminate with a single delamination located at an arbitrary location along the length and through the thickness.

The single delamination subdivides the laminate into four regions (see Fig. 1). The formulation makes use of equilibrium equations, continuity requirements at the crack tips and boundary conditions at the ends. The post-buckling analysis, derived by variation principles, assumes an imperfect system. Then the new set of relations for the energy release rate and the mode mixity in a laminate with an arbitrary stacking sequence are briefly summarized. A general computer code is developed and used to study the effect of a wide range of parameters.

POST-BUCKLING ANALYSIS

Let (χ, y) be the coordinate of the reference surface and z the normal coordinate (Fig. 1). Application of Kirchoff-Love hypothesis and resorting to the Von-Karman non-linear kinematic approach, results in the following relations for the one dimensional model (in x and z):

$$\begin{aligned} \varepsilon_{xx}(x,z) &= \bar{\varepsilon}_{xx}(x) + z\phi_{xx}(x) \\ \bar{\varepsilon}_{xx}(x) &= u(x)_{,x} + \tfrac{1}{2} w(x)_{,x}(w(x)_{,x} + 2\bar{w}(x)_{,x}) \\ \phi_{xx}(x) &= -w(x)_{,xx}. \end{aligned} \tag{1}$$

$\bar{\varepsilon}$ and ϕ are, respectively, the strain of the reference surface and the change of curvature under the displacement field in the axial ($u(x)$) and normal ($w(x)$) directions, associated with the imperfection function $\bar{w}(x)$. The imperfection function is the initial, normal displacement at the unloaded state. The reference surfaces, e.g. (zr_i), are defined by:

$$\sum \int_z c_{xx}\bar{z}\,\mathrm{d}\bar{z} = \left(\sum \int_z c_{xx}\,\mathrm{d}\bar{z}\right)(zr_i)$$

where $\bar{z}$ is the normal coordinate from the top surface of each region.

Under the classical laminate theory, the constitutive equations can be written as (see Sheinman and Kardomateas, 1997):

$$\begin{aligned} \bar{\varepsilon}_{xx} &= \alpha_1 N_{xx} + \alpha_2 M_{xx} \\ \phi_{xx} &= \alpha_3 N_{xx} + \alpha_4 M_{xx}. \end{aligned} \tag{2}$$

N_{xx} and M_{xx} are the axial force and bending moment of the one dimensional model: α_i are derived from the theory of the one-dimensional model.

For classical beam theory:

$$\begin{aligned} \alpha_1 &= D_{11}/(\gamma A_{11}) \\ \alpha_2 &= \alpha_3 = -B_{11}/(\gamma A_{11}) \\ \alpha_4 &= 1/\gamma \\ \gamma &= D_{11} - B_{11}^2/A_{11} \\ (A_{11}, B_{11}, D_{11}) &= \int c_{xx}(1, z, z^2)\,\mathrm{d}z \end{aligned} \tag{3}$$

where

$$\begin{aligned} c_{xx} &= Q_{11} + \delta(c_1 Q_{12} + c_2 Q_{23}) \\ c_1 &= (Q_{23}Q_{13} - Q_{33}Q_{12})/(Q_{22}Q_{33} - Q_{23}^2) \\ c_2 &= (Q_{23}Q_{12} - Q_{22}Q_{13})/(Q_{22}Q_{33} - Q_{23}^2) \\ \delta &= \begin{cases} 0 & \text{for plane strain} \\ 1 & \text{for plane stress} \end{cases} \end{aligned} \tag{4}$$

Q_{ij} are the reduced laminate transformed stiffness coefficients.

For cylindrical bending theory (see also Sheinman, 1989);

$$\begin{aligned} \alpha_1 &= \{[I + A^{-1}BGB]A^{-1}\}_{11} \\ \alpha_2 &= \{-A^{-1}BG\}_{11} \\ \alpha_3 &= \{-GBA^{-1}\}_{11} \\ \alpha_4 &= \{G\}_{11} \\ G &= (D - BA^{-1}B)^{-1} \\ (A_{ij}, B_{ij}, D_{ij}) &= \int Q_{ij}(1, z, z^2)\,\mathrm{d}z \quad (i,j = 1,2,3). \end{aligned} \tag{5}$$

The subscript $(\ )_{11}$ means the first term of the matrix. It is seen that the α's are determined not only by A_{11}, B_{11}, D_{11} but also by A_{ij}, B_{ij}, and D_{ij} $i, j = 1, 2, 3$.

The delamination subdivides the laminate into four regions (Fig. 1) for which the nonlinear equilibrium equations are derived by the following variational principle:

$$\delta\pi = \sum_{j=1}^{4} \delta\pi_B^j + \sum_{k=1,4} \delta\pi_N^k + \delta\pi_c = 0. \tag{6}$$

$\delta\pi_B^j$ is the variation of the total potential energy at region j:

$$\delta\pi_B^j = \int_{x_0^j}^{x_c^j} \left\{ \eta^j \left[-\alpha_4^j \left(u_{,x}^j + \frac{1}{2} w_{,x}^j (w_{,x}^j + 2\bar{w}_{,x}^j) \right) - \alpha_2^j w_{,xx}^j \right] [\delta u_{,x}^j + (w_{,x}^j + \bar{w}_{,x}^j)\delta w_{,x}^j] \right.$$
$$\left. - \eta^j \left[\alpha_3^j \left(u_{,x}^j + \frac{1}{2} w_{,x}^j (w_{,x}^j + 2\bar{w}_{,x}^j) \right) + \alpha_1^j w_{,xx}^j \right] \delta w_{,xx}^j - q_x^j \delta u^j - q_z^j \delta w^j \right\} \mathrm{d}x. \tag{7}$$

x_o^j and x_c^j are the coordinates of the ends of the region j. q_x and q_z are the external applied distributed loads in axial and transverse direction and $\eta = 1/(\alpha_2\alpha_3 - \alpha_4\alpha_1)$.

π_N^k is the functional expressing the continuity conditions at the crack tip k ($k = 1$ for the first tip and $k = 4$ for the second tip):

$$\pi_N^k = \left\{ \lambda^{(k_1)} \left(u^{(2)} - u^{(k)} + \frac{h}{2} w_{,x}^{(k)} \right) + \lambda^{(k_2)} \left(u^{(3)} - u^{(k)} - \frac{H}{2} w_{,x}^{(k)} \right) + \lambda^{(k_3)} (w^{(2)} - w^{(3)}) \right.$$
$$\left. + \lambda^{(k_4)} (w^{(3)} - w^{(k)}) + \lambda^{(k_5)} (w_{,x}^{(2)} - w_{,x}^{(3)}) + \lambda^{(k_6)} (w_{,x}^{(3)} - w_{,x}^{(k)}) \right\} \Bigg|_{x = x^{(k)}}. \tag{8}$$

$\lambda^{(k_i)}$ are the Lagrange multipliers, $x^{(1)}$ and $x^{(4)}$ the coordinates of the first and second crack tips, respectively. The first two terms express the axial displacement compatibility, the next two terms the transverse displacement and the last two terms the slope continuity between the delaminated layer (3) and the substrate (2) at their common sections, which are at the locations of the delamination tips.

Finally, π_c is the functional which is used for imposing the geometrical compatibility through another Lagrange multiplier Λ, for the contact constraints between region $j = 2$ and $j = 3$:

$$\pi_c = \int_{x_0^2}^{x_c^2} \Lambda (w^{(3)} - w^{(2)}) \, \mathrm{d}x. \tag{9}$$

Minimization of the functional (eqn 6) yields nonlinear differential equations for the pre- and post-buckling states. The Newton's method is employed for reducing the nonlinear equations to a linear sequence, and a central finite-difference scheme (as in Sheinman *et al.*, 1989) to convert the differential equations into algebraic ones.

DELAMINATION GROWTH

A combined fracture mechanics analysis and delamination post-buckling solution is needed for studying the growth characteristics of the delamination. The post-buckling analysis has just been presented and the fracture mechanics approach is basically based on a Griffith type criterion. Notice that the growth is assumed to occur between composite layers, rather than through the layers.

It is important to examine whether the delamination growth, under a given load level, is stable or unstable (see Kardomateas and Pelegri, 1994). Delamination growth depends on the level of the energy release rate, at the crack tip. Another important quantity affecting growth is the mode mixity (see Hutchinson and Suo (1992), Kardomateas *et al.* (1995) for cyclic loading). In essence, the toughness does not have a single value, it is rather a function of the relative amount of Mode II to Mode I acting on the interface. A set of relations for decomposition of the energy release rate into Mode I and Mode II has been recently

developed for an arbitrary stacking sequence composite laminate, by Sheinman and Kardomateas (1997). It is adopted for the study of delamination growth in the post-buckling stage and briefly summarized here.

For any load level, first the post-buckling state is analyzed, then the energy release rate at the crack tips is computed by J-integral and given by:

$$G = \frac{1}{2}\left[\frac{P_u^2}{R_1} + \frac{M_u^2}{R_2} + \frac{2G_{pm}}{\sqrt{R_1 R_2}}\right] \tag{10}$$

where P_u and M_u are the relevant axial force and bending moment of the delaminated part (see Fig. 2) which are computed by the stress superposition (see Sheinman and Kardomateas, 1997), and R_1, R_2, G_{pm}, γ are constants defined by:

$$\begin{aligned}
\frac{1}{R_1} &= \alpha_1^{(2)} + \alpha_1^{(3)} - (\alpha_2^{(2)} + \alpha_3^{(2)})(h - z_{r2} - z_{r3}) + a_4^{(2)}(h + z_{r2} - z_{r3})^2 \\
\frac{1}{R_2} &= \alpha_4^{(2)} + \alpha_4^{(3)} \\
G_{pm} &= P_u M_u \sin\gamma \\
\sin\gamma &= \frac{\sqrt{R_1 R_2}}{2}[\alpha_2^{(2)} + \alpha_2^{(3)} + \alpha_3^{(2)} + \alpha_3^{(3)} - 2\alpha_4^{(2)}(h + z_{r2} - z_{r3})].
\end{aligned} \tag{11}$$

$\alpha_i^{(2)}$ and $\alpha_i^{(3)}$ $(i = 1, 2, 3, 4)$ are the coefficients, given by eqn (3) or (5), of the substrate region $(j = 2)$ and the delaminated region $(j = 3)$, respectively. z_{r2} and z_{r3} are the reference surfaces of regions $j = 2$ and $j = 3$, respectively.

Decomposition of the energy release rate yields:

$$\begin{aligned}
G_I &= p_{11} n \lambda^{-3/4} K_I^2 \\
G_{II} &= p_{11} n \lambda^{-1/4} K_{II}^2
\end{aligned} \tag{12}$$

where

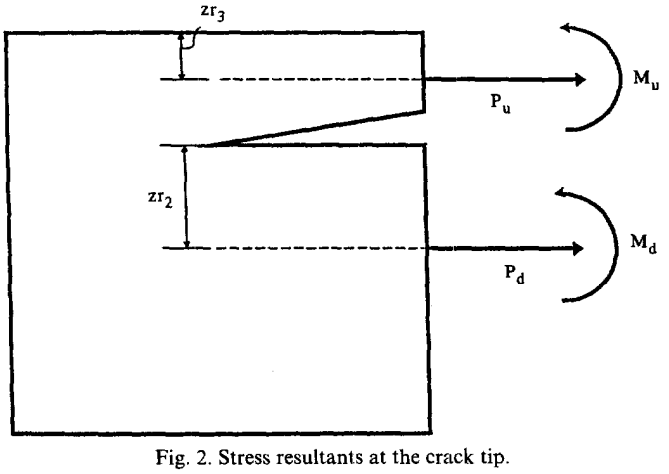

Fig. 2. Stress resultants at the crack tip.

$$n = \sqrt{\frac{1+\rho}{2}}$$

$$\rho = \frac{2p_{12}+p_{33}}{2\sqrt{p_{11}p_{22}}}$$

$$\lambda = p_{11}/p_{22}$$

$$K_I = \frac{\lambda^{3/8}}{\sqrt{2p_{11}n}}\left[\frac{P_u}{\sqrt{R_1}}\cos\omega \pm \frac{M_u}{\sqrt{R_2}}\sin(\omega+|\gamma|)\right]$$

$$K_{II} = \frac{\lambda^{1/8}}{\sqrt{2p_{11}n}}\left[\frac{P_u}{\sqrt{R_1}}\sin\omega \mp \frac{M_u}{\sqrt{R_2}}\cos(\omega+|\gamma|\right]. \tag{13}$$

p_{ij} are the coefficients of the compliance matrix in the x-z plane; ω is a function of the material and geometric parameter, approximately given by $\omega = 52.1\text{-}3h/H$ (in degrees) as is suggested by Suo (1990). The upper signs of M_u (in K_I and K_{II}) is for the case of $G_{pm} > 0$ and the lower for case of $G_{pm} < 0$.

PARAMETRIC STUDY

The post-buckling analysis with delamination growth is implemented into a general purpose computer code. It covers the non-linear behavior of any laminated composite with a single delamination located at an arbitrary location along the length and through the thickness. The code is an extension of Sheinman *et al.* (1989) and Sheinman and Soffer (1991), to include an arbitrary located delamination as well as delamination growth according to the criteria given by Sheinman and Kardomateas (1997). It is used here for a parametric study of delamination growth during the pre- and post-buckling stages. Emphasis is given to the growth characteristics of the delamination, rather than to the deformation pattern during the post-buckling phase. Examples of isotropic and composite laminates under axial compression are considered for the parametric study.

ISOTROPIC CASE

The delamination growth is initially examined in a clamped isotropic beam, taken from Sheinman and Soffer (1991): length-to-thickness ratio $l/t = 50$ modulus of elasticity $E = 2.1\ 10^{11}$ N/m^2, Poisson's ratio $\nu = 0.3$. The initial imperfection is assumed to be

$$\bar{w}(x) = \frac{\delta_0}{2}\left(1-\cos\frac{2\pi x}{l}\right).$$

The energy release rate versus symmetric delaminated length ($l_1 = l_4$) for delamination thickness $h/t = 0.1$ and amplitude of imperfection $\delta_o/t = 0.02$, is plotted in Fig. 3 for several values of the axial load N/N_{cr} (N is the applied axial load and N_{cr} is the buckling load of the perfect undelaminated beam). It seems that the growth may start from $l_2/l \geqslant h/t$, that the critical length for unstable-to-stable transition of the delamination is $l_2/l_3 \cong 0.3$ and that the growth (if occurs at all) is unstable up to $l_2/l = 0.3$. The effect of imperfection amplitude and of the thickness of the delaminated part are shown in Fig. 4. The mode mixity, defined by $\psi = \tan^{-1}(K_{II}/K_I)$ is a very important parameter for growth (Kardomateas, 1995). This quantity for the first and second tip for unsymmetrical delaminated laminate ($l_1 \neq l_4$) is plotted in Fig. 5.

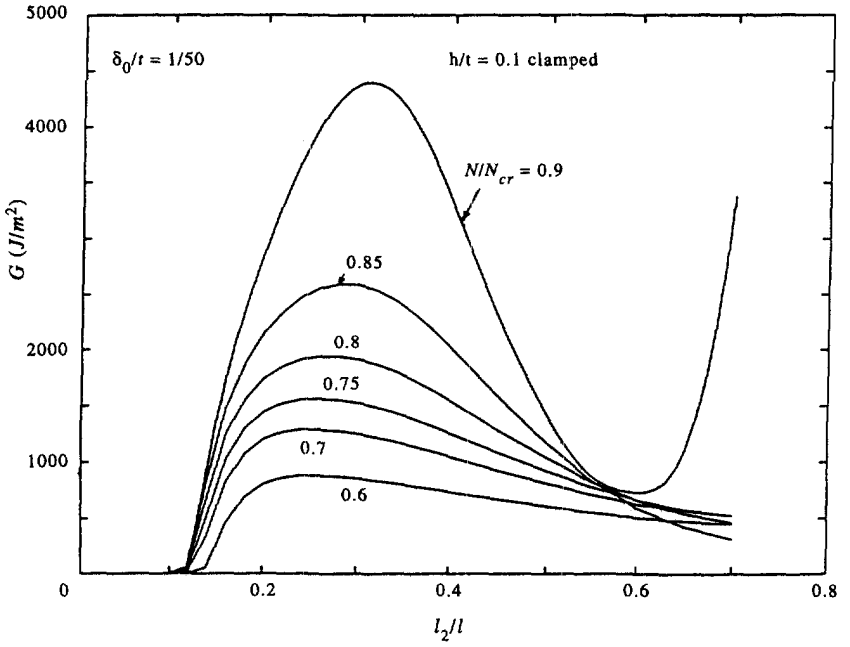

Fig. 3. Energy release rate versus delamination length for isotropic delaminated laminate.

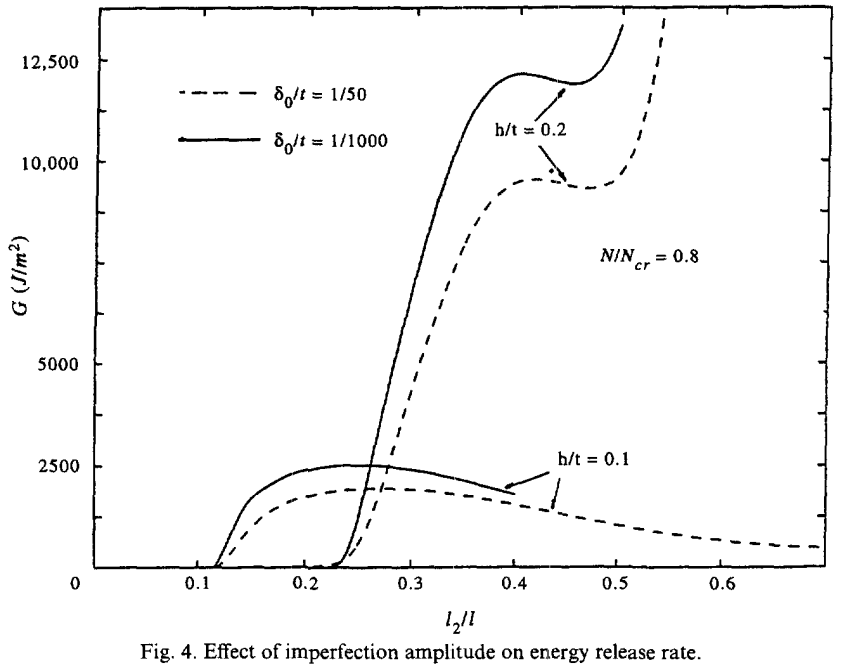

Fig. 4. Effect of imperfection amplitude on energy release rate.

COMPOSITE LAMINATE

This example concerns a graphite/epoxy C30/922 delaminated clamped beam under axial compression. The data for this example are taken from Kardomateas *et al.* (1995) and from Pelegri *et al.* (1995): length $l = 0.09652$ m, width $b = 0.0127$ m, thickness of laminate $t = 0.0013335$ m, 15-ply laminate with $h_{ply} = 8.89\ 10^{-5}$ m, $E_{11} = 137.9\ 10^9$ N/m^2, $E_{22} = 8.98\ 10^9$ N/m^2, $G_{12} = 7.2\ 10^9$ N/m^2, $\nu_{12} = 0.3$. Mode I and II critical energy release rates: $G_I^c = 190$ J/m^2, $G_{II}^c = 630$ J/m^2. Symmetric stacking combination of $[0,(\alpha/-\alpha)_6,\alpha,0]$ with various angle values α and cross-ply $[0,(90/0)_7]$ were chosen. A delamination of length $l_2 = 0.0508$ m with symmetric location ($l_1 = l_4$) was chosen to be located between the 4th

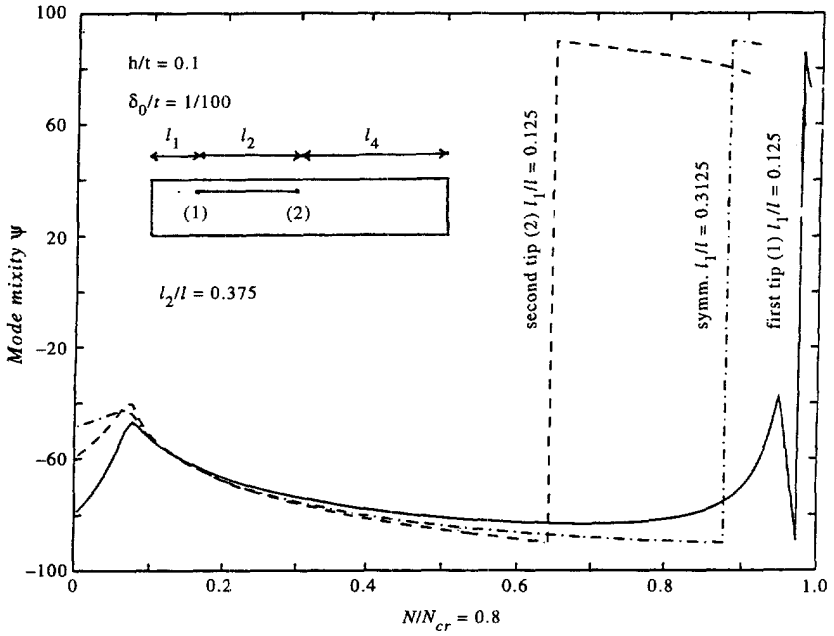

Fig. 5. Mode mixity for unsymmetrical delaminated isotropic laminates.

and the 5th layer. It should be mentioned that, because of the delamination, the layup of region 3 $(\alpha/-\alpha)_2$ is asymmetric and, therefore, bending stretching coupling is active.

The internal axial load, using plane strain theory, at the delaminated region ($j = 3$) versus the total axial load N/N_{cr} for different α-orientation is plotted in Fig. 6. N_{cr} is defined as the critical load of the perfect (undelaminated) unidirectional laminate $[0]_{15}$. The local buckling load, defined as the load for buckling of the delamination (as opposed to the global buckling load, which is defined as the load for buckling of the entire beam), which is clearly observed, is significantly affected by the α parameter, the larger α, the lower the critical load. The post-buckling behavior (given by the midpoint displacements of the

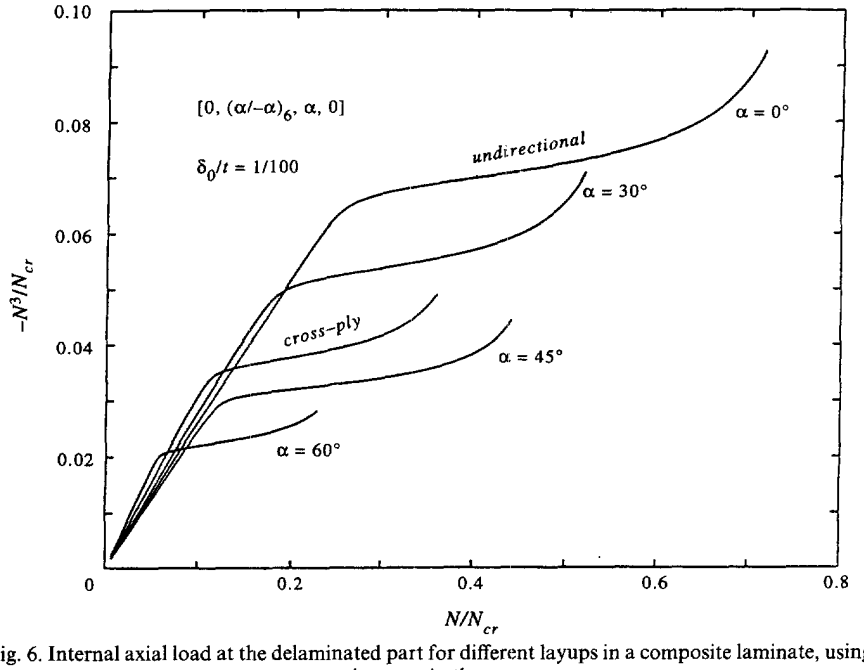

Fig. 6. Internal axial load at the delaminated part for different layups in a composite laminate, using plane strain theory.

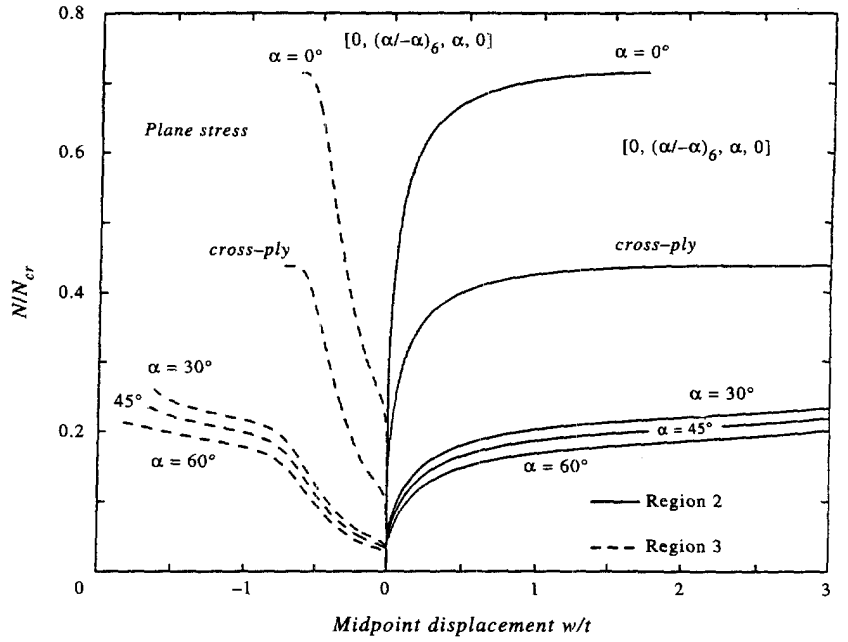

Fig. 7. Post-buckling displacement curves based on plane stress theory.

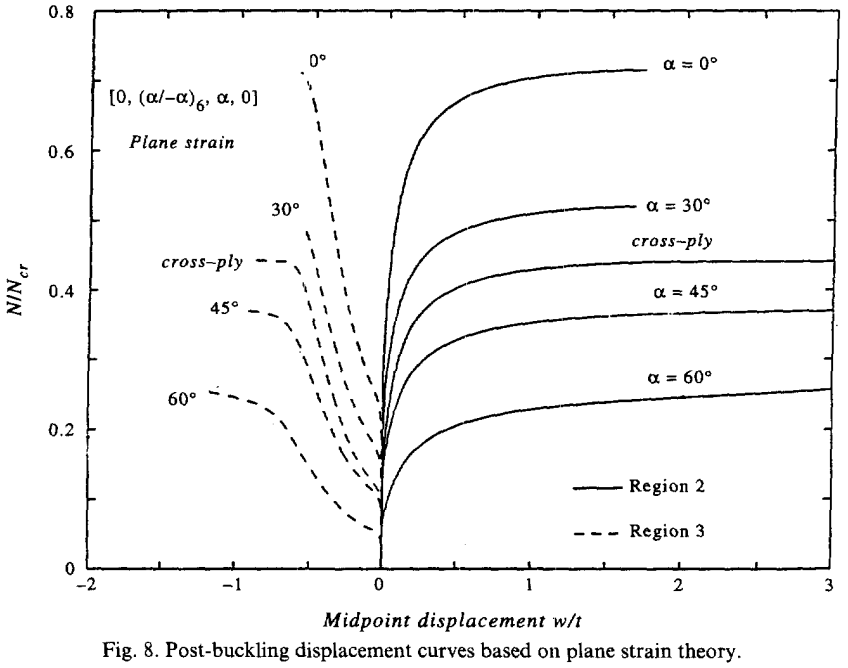

Fig. 8. Post-buckling displacement curves based on plane strain theory.

substrate region ($j = 2$) and of delaminated region ($j = 3$) is shown in Figs 7 and 8, respectively, for plane stress and plane strain. It seems that the plane stress (suitable for a narrow beam) yields much lower local and global buckling load than the plane strain (suitable for a wide beam) and there is no significant difference for the range of angle $\alpha = 30° \div 60°$, unlike the plane strain case. For $\alpha = 0°$ and for cross-ply the results of the two theories are the same. The effect of the theory type on the mode mixity is given in Fig. 9 for $\alpha = 45°$. As expected, the cylindrical bending theory is closer to the plane strain one.

Figure 10 shows the energy release rate G, G_I and G_{II} for cross-ply and unidirectional laminates. The total energy release rate (G) of the cross-ply layup, for different depths of the delamination, is plotted in Fig. 11 (there N_{cr} is the critical load of the perfect cross-ply laminate). It is clear that the worst location, from delamination growth point of view, is

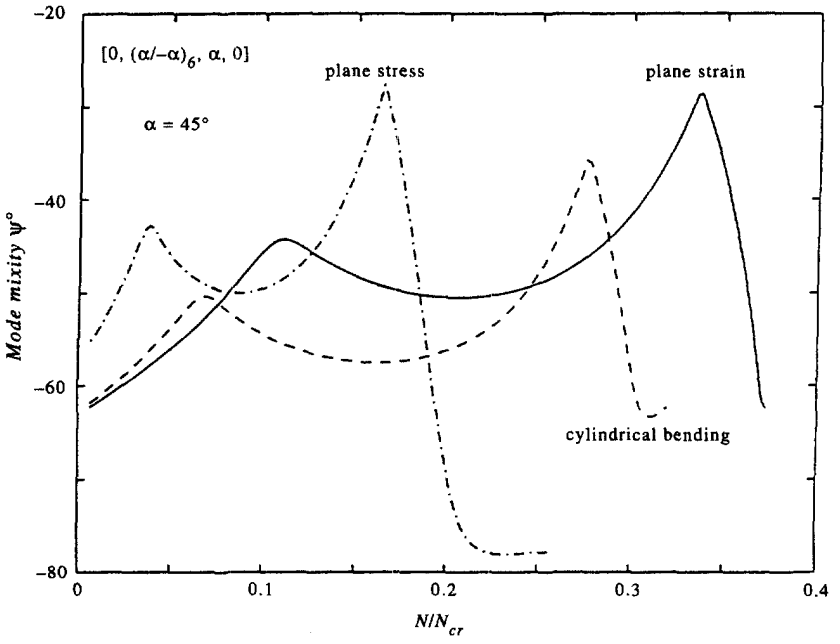

Fig. 9. Mode mixity for composite layup $[0,(45/-45)_6 45, 0]$ (different theories).

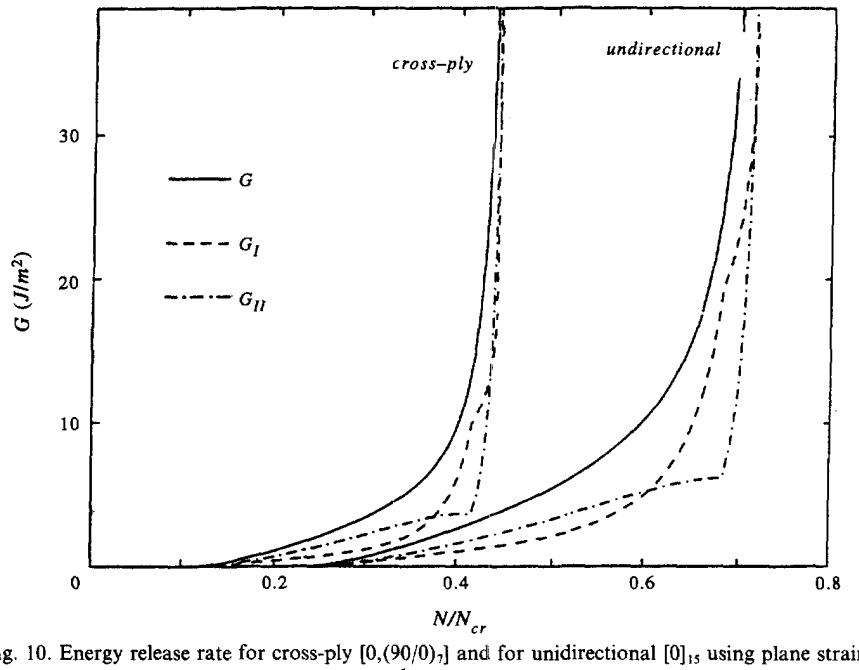

Fig. 10. Energy release rate for cross-ply $[0,(90/0)_7]$ and for unidirectional $[0]_{15}$ using plane strain theory.

between the 4th and the 5th layer. It seems that G is increasing with the depth up to 4/5 and then decreasing. The total energy release rate is the same for delamination between layer 1 and 2, between 2 and 3, and so on, because of the fact that the 90° plies contribute very little ($E_{22}/E_{11} \cong 1/15$). It is also clear that, for this case, there is no delamination growth (the energy release rate is much lower than $G^c(\psi)$). The mode mixity ψ versus the load level, for several α's-orientation, is given in Fig. 12. The local and global buckling loads are clearly observed.

Finally, the effect of the l/t ratio on the energy release rate, is studied for unidirectional delaminated laminates. For this case $t = 0.0013335$ m, $l_2/l = 0.526$ and $h/t = 4/15$ were kept constant, which yields the same non-dimensional local ($N^{\text{local}}/N_{cr} = 0.257$) and global

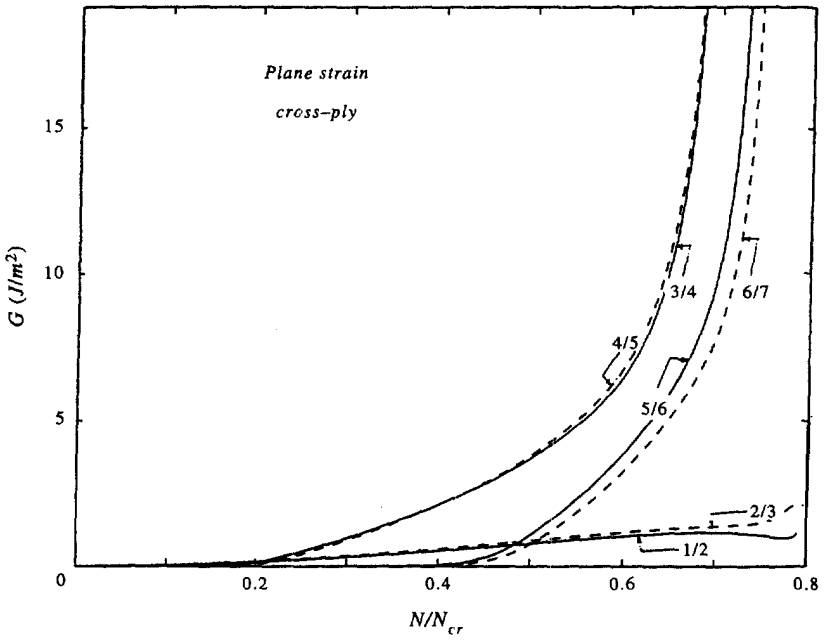

Fig. 11. Effect of delamination depth on the energy release rate for cross-ply laminate.

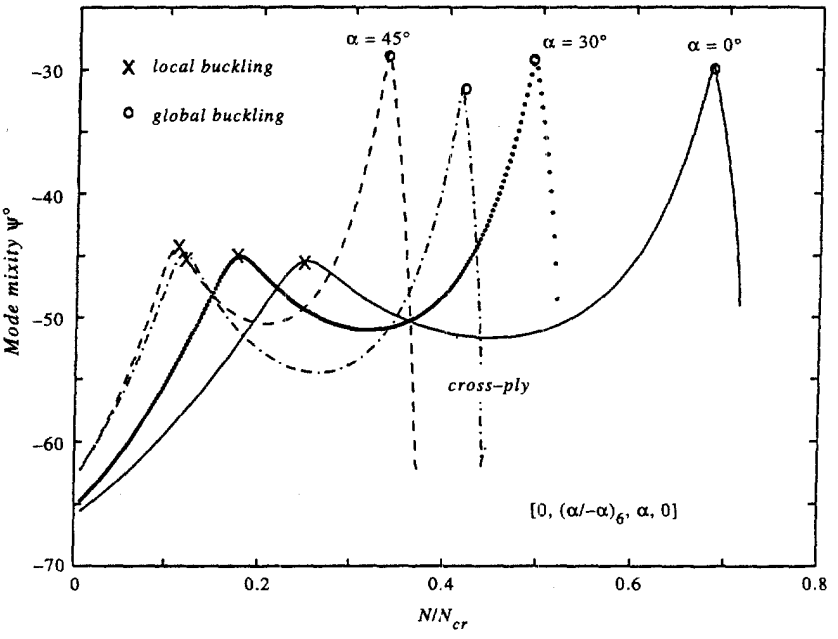

Fig. 12. Mode mixity for composite laminates.

($N^{\text{global}}/N_{cr} = 0.715$) buckling load ($N_{cr}$ is the global buckling load of the perfect unidirectional specimen). N^{local} and N^{global} are, respectively, the externally applied axial loads, which would cause the local and global buckling modes. The semilogarithmic curves of energy release rate for different l/t ratios are plotted in Fig. 13. It is clearly observed that l/t is a dominant parameter in terms of energy release rate. The lower the l/t ratio, the higher (in scale order) the energy release rate. For the given material toughness of $G^c = 190$ J/m^2 (assuming that $G^c(\psi) = G_I^c$ is conservative) there is no delamination growth for a high l/t ratio. For $l/t = 30$ the growth starts far away beyond the local buckling point, while for $l/t = 10$ it starts even below the local buckling load. Experimental agreement of no delamination growth for $l/t = 72.4$ and for $l/t = 37.4$ can be found in Kardomateas *et al.* (1995) and Pelegri *et al.* (1995).

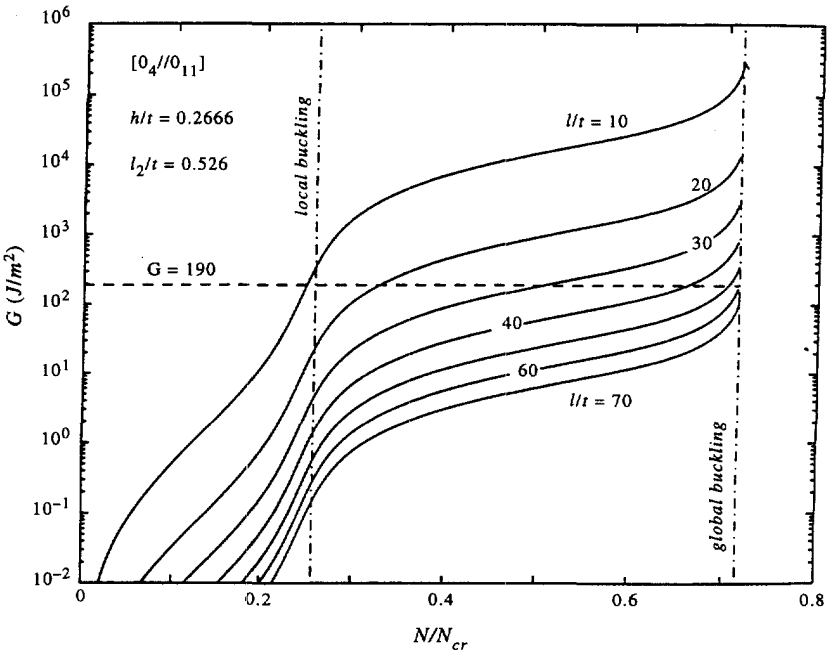

Fig. 13. Effect of length-to-thickness ratio l/t on the energy release rate for unidirectional laminate.

CONCLUSION

An analytical procedure for studying delamination growth during the pre- and post-buckling stages of a single delaminated composite laminate is performed. The theory and the solution procedure are general for any arbitrary non-linear one-dimensional model of a composite laminate under external loading. A new set of relations for the energy release rate and the mode mixity in a delaminated laminate with an arbitrary stacking sequence is implemented. A study of a wide range of parameters was carried out, and of the principal findings the following should be emphasized:

1. The post-buckling behavior of delaminated composite laminates is strongly affected by the delamination growth.
2. For length-to-thickness ratio, on which the classical plate assumptions are held—there is no need of 3-dimensional analysis for delamination growth.
3. The delamination length plays the most important role regarding stable or unstable growth.
4. The chosen imperfection function may affect the post-buckling behavior because of the contact phenomenon. For some imperfection modes and amplitudes no contact occurs.
5. Depending on the theory type used, i.e. plane stress, plane strain and cylindrical bending, and on the layup sequence, significant differences may be observed.
6. Growth of the delamination is mostly affected by the length-to-thickness, l/t, ratio (for constant h/t and l_2/l ratios, where l is the specimen length, also see Fig. 1).
7. Delamination growth takes place under mixed mode, characterized by a relatively high value of Mode II, especially beyond the load level of local buckling.

Acknowledgements—The financial support of the Office of Naval Research, Ship Structures S&T Division, Grant N00014-91-J-1892, and of the Army Research Office through CERT, Grant NCC2-945, and the interest and encouragement of the Grant Monitors Dr Y. D. S. Rajapakse and Dr G. Anderson, are both gratefully acknowledged. The research was also partially supported by the fund for the promotion of research at the Technion through the first author.

REFERENCES

Chai, H., Babcock, C. D. and Knauss, W. G. (1981) One dimensional modeling of failure in laminated plates by delaminations buckling. *International Journal of Solids and Structures* **27**(11), 1069–1083.

Hutchinson, J. W. and Suo, Z. (1992) Mixed mode cracking in layered materials. In *Advances in Applied Mechanics*, Vol. 28. Academic Press, New York.

Kardomateas, G. A. (1993) The initial post-buckling and growth behavior of internal delaminations in composite plates. *ASME Journal of Applied Mechanics* **60,** 903–910.

Kardomateas, G. A. and Pelegri, A. A. (1994) The stability of delamination growth in compressively loaded composite plates. *International Journal of Fracture* **65,** 261–276.

Kardomateas, G. A., Pelegri, A. A. and Malik, B. (1995) Growth of internal delaminations under cyclic compression in composite plates. *Journal of Mechanics and Physics of Solids* **43**(6), 847–868.

Kultz, Z. and Chang, F. K. (1992) Modeling compression failure of laminated composites containing multiple through the width delaminations. *Journal of the Composite Materials* **26**(3), 350–387.

O'Brien, T. K. (1982) Characterization of delamination onset and growth in a composite laminate. In *Damage in Composite Materials ASTM STP* 775 ed. K. L. Reifsnider. American Society for Testing and Materials, pp. 140–167.

Pelegri, A. A., Kardomateas, G. A. and Malik, B. U. (1997) The fatigue growth of internal delaminations under compressive loading in cross ply composite plates. In *Composite Materials: Fatigue and Fracture* sixth volume, ASTM 1285 ed. E. A. Armanios. American Society for Testing and Materials, Philadelphia, pp. 146–163.

Sallam, S. and Simitses, G. J. (1985) Delamination buckling and growth of flat cross-ply laminates. *Composite Structures* **4,** 361–381.

Sheinman, I. (1989) Cylindrical buckling load of laminated columns. *Journal of Engineering Mechanics, ASCE* **115**(3), 659–661.

Sheinman, I., Bass, M. and Ishai, O. (1989) Effect of delamination on stability of laminated composite strip. *Composite Structures* **11**(3), 227–242.

Sheinman, I. and Soffer, M. (1991) Post-buckling analysis of composite delaminated beams. *International Journal of Solids and Structures* **27**(5), 639–646.

Sheinman, I. and Kardomateas, G. A. (1997) Energy release rate and stress intensity factors for delaminated composite laminates. *International Journal of Solids and Structures* **34**(4), 451–459.

Suo, Z. (1990) Delamination specimens for orthotropic materials. *ASME Journal of Applied Mechanics* **57,** 627–634.

Whitcomb, J. D. (1989) Three-dimensional analysis of a post-buckling embedded delamination. *Journal of Composite Materials* **23,** 862–889.